Reprinted from the Preprint Volume of the **Seventh Conference on Applied Climatology**, September 10-13, 1991, Salt Lake City, Utah. Published by the American Meteorological Society, Boston, Mass.

4B.5

Satellite-based Convective Climatologies over the Florida Peninsula

Stephan B. Smith, Patrick N. Dills, John F. Weaver, and James F.W. Purdom

NOAA/NESDIS Regional and Mesoscale Meteorology Branch, Cooperative Institute for Research in the Atmosphere, Colorado State University (CIRA), Fort Collins, Colorado

1. Introduction

Mesoscale solenoidal circulations can play a fundamental role in determining the location and strength of cumulus convection in regions where differences in vegetation, land use and/or topography are great. Such circulations, initiated by differential surface heating, are modified by the large-scale flow regimes in which they form. Klitch et al. (1985) showed that convective climatologies derived from visible and infrared geostationary satellite imagery are viable tools for studying the diurnal evolution of convection and precipitation associated with the mountain plains solenoidal circulation in Colorado. Gibson and Vonder Haar (1990) used a similar technique to examine how the convective cloud development in the southeastern United States is influenced by small-scale geographic features and the solenoids which form along them (e.g. sea, lake, river, and bay breezes).

Blanchard and Lopez (1985) and Michaels et al. (1987) constructed radar composites of the daily evolution of sea-breeze convection in Florida for a variety summertime synoptic flow patterns. Both these studies revealed distinct patterns in convective development which varied according to the large-scale environment. However, since echoes of radar reflectivity indicate precipitating storms, convective climatologies based on conventional radar miss the important pre-storm organization along the sea-breeze convergence zone which in satellite imagery appears as a thin line of rapidly growing non-precipitating cumulus. From the perspective of a forecaster, an understanding of the pre-storm phase of convective development is crucial in order to provide a timely and accurate nowcast of thunderstorm occurrence.

The goal of this study is to use satellite-based convective climatologies in an attempt to understand (1) how and where the sea-breeze circulation interacts with the different synoptic flow patterns to trigger convection in Florida and (2) if and how this interaction determines where the convection will move. McQueen and Pielke had similar objectives in their 1985 study. Their composites, stratified by surface geostrophic wind speed and direction, resembled the radar composites of Michaels et. al (1987) and mesoscale modeling studies cited in Pielke et al. (1991). However, the sample size of 39 days from which the composites were computed was too small to provide statistically significant results. Though the composites presented in this paper are based on only 38 more days than used by McQueen and Pielke (1985), they are being updated through an ongoing collection of GOES imagery over Florida to provide a sample size sufficient for significant results and to examine the role of seasonal variability.

2. Methodology

An hourly 1500-2100 UTC sequence of visible (VIS) 2 km resolution and infrared (IR) 4 km resolution GOES satellite digital imagery over Florida was collected on 77 days from August 2 through October 18, 1990. Simple VIS composites were made by averaging the visible count at each pixel over many images for all of Florida and surrounding coastal waters. Further processing of the visible imagery involved attempting to produce actual counts of cloud frequency. This was done by first constructing lowest pixel base images for each hour studied (1500-2100 UTC). These images are composed of the lowest brightness value observed at a each pixel location and thus represent hourly cloudless visible images of Florida. Each individual image then was compared with its corresponding lowest pixel image. Pixels brighter than a given brightness threshold above the mean pixel value of each base image were assigned a value of 1 for cloud. Pixels darker than the selected threshold were set to 0 for no-cloud. In this manner, the effect of visible radiation reflected off of cloud-free land and water surfaces is removed. These composites thus show the frequency of occurrence of clouds brighter than a selected brightness. Similarly, the IR composites display the frequency of occurrence of clouds colder than a selected threshold temperature.

In the composites constructed using all days during the sample period the influence of different synoptic flow regimes largely disappears, and the average sea-breeze forcing is evident. The task of separating the synoptic effects from local forcing was handled by first stratifying each day by its predominant boundary layer flow direction and recalculating the hourly composites for each direction. The directions chosen were northerly (N, 5 days), northeasterly (NE, 21 days), easterly (E, 11 days), southeasterly (SE, 8 days), southerly (S, 6 days), southwesterly (SW, 18 days), westerly (W, 1 day) and northwesterly (NW, 7 days). The flow direction was subjectively determined by looping the VIS imagery for each day and observing the orientation of the cloud-free lake shadow downwind of Lake Ockeechobee and other bodies of water in the region. For this reason the stratifications are only valid for the part of the peninsula south of Cape Canaveral. The lake shadow wind direction usually agreed with the 12 UTC, 850 mb wind direction observed at Tampa Bay to within plus or minus 45 degrees.

3. Results

For brevity only the cloud frequency composites derived from VIS imagery are presented. The brightness threshold was set such that small cumulus clouds would be included in the composites while very thin cirrus and stratus would be excluded. We first examine the mean sea-breeze forcing seen on the 15, 18, and 20 UTC composites computed for all days. At 15 UTC (Fig. 1a; composed of 60 images), the highest frequencies (> 40%) occur mostly over water associated with the remnants of nocturnal land-breeze convection and/or other disturbances (e.g. fronts, mesoscale thunderstorm clusters, etc.). Local maxima over land are found along the southeast coast near Miami and along the northwest coast south of the panhandle. Lake Ockeechobee appears as a local minimum. At 18 UTC (Fig. 1b; composed of 63 images), cloud frequency has diminished over the water and increased over the peninsula as the offshore subsidence and onshore rising motion, driven by the sea-breeze circulation, intensify. In general frequencies over land are highest near the coastline associated with the sea-breeze convergence zone. Ockeechobee persists as a relatively cloud sparse area. By 20 UTC (Fig. 1c, composed of 59 images) the highest frequencies (60-70%) are located slightly inland of the southwestern coast in agreement with the findings of Blanchard and Lopez (1985) and Michaels et al. (1987). A secondary maximum (≃ 50%) east of Okeechobee may indicate cloudiness induced by vertical motion formed by the frequent collision of the east coast sea-breeze and Ockeechobee lake-breeze. Though still a local minimum, cloud frequencies over Okeechobee are higher at this time probably due to the presence of thicker cirrus anvils associated with surrounding mature thunderstorms. In all three images, cloud frequencies are higher over the Atlantic than over the Gulf of Mexico. The causes for the greater cloud frequencies over the Atlantic are not yet clear.

The influence of the synoptic environment on diurnal sea-breeze convective development can be seen by examining the 15,18, and 20 UTC composites of the most common flow regimes for our dataset, SW and NE. The 15-18-20 UTC sequence for SW flow days (Fig. 2; composed of 17, 16 and 13 images respectively) shows that local maxima in cloud frequencies move from the southwest coast to the east coast during the course of the day and in the same general direction as the low-level winds. A band of high cloud frequencies stretching from the Gulf of Mexico to the Atlantic across the northern half of the peninsula indicates cloudiness associated with a synoptic front. Such a front was present on 15 out of 18 days in the SW sample set. Low frequencies off the east coast indicate enhancement of the east coast sea breeze subsidence zone. The Ockeechobee shadow is evident where relatively lower frequency counts extend northeast of the lake.

In contrast to the SW case, the 15-18-20 UTC sequence for NE flow (Fig. 3, composed of 16, 18, and 18 images respectively) displays a shift in cloudiness from the east coast to the southwest coast from morning to late afternoon. The shift in cloud frequency from one coast to another is in agreement with the numerical modelling experiments of Pielke (1974) and the radar climatologies of Blanchard and Lopez (1985). These studies found that the sea-breeze on the upwind coast quickly moves inland with the synoptic flow while the sea-breeze on the downwind coast progresses at a slower rate, sometimes remaining quasi-stationary. Analogous to the SW case, the west coast sea breeze subsidence zone appears to be enhanced by the prevailing NE flow. The Okeechobee shadow is again evident from the local cloud frequency minimum this time present on the southwest side of the lake. Notice should be taken of the band of higher frequencies along the southern edge of the shadow boundary at 20 UTC. Individual case day images often show the shadow edge as a preferred region of cloud development.

4. Conclusions

Composited imagery reveals significant patterns in both formation and movement of convection particular to different synoptic flow regimes. In the mean one can clearly see that sea-breeze circulations and other smaller solenoidal circulations play an important role in development of convection over Florida. However, a careful examination of the day-to-day imagery from which the composites were constructed showed that many other factors may significantly modify or even override this role.

As mentioned above, the collection of GOES VIS and IR image data over Florida at CIRA is continuing. As the sample size becomes very large synoptic variation would be expected to "average out" nearly completely. The composites would then show local maxima in cloud frequency attributable solely to the diurnal forcing of the sea-breeze and other smaller-scale solenoids. Such composites could be used in the interpretation of cloud patterns in real-time satellite imagery, keeping in mind the daily variations brought about by transient synoptic and mesoscale disturbances. The results also have direct application to the initialization and verification of mesoscale numerical weather prediction models, as well as in the study of microscale climate and climatic variations, particularly with respect to cloud cover and precipitation.

ACKNOWLEDGEMENTS

This research was supported by NOAA NA85RAH05045.

REFERENCES

Blanchard, D.O., and R.E. Lopez, 1985: Spatial patterns of convection in South Florida, Mon. Wea. Rev., 113, 1282-1299.

Gibson, H.M., and T.H. Vonder Haar, 1990: Cloud and convection frequencies over the southeast United States as related to small-scale geographical features, Mon. Wea. Rev., 118, 2215-2227.

Klitch, M.A., J.F. Weaver, F.P. Kelly, and T.H. Vonder Haar, 1985: Convective cloud climatologies constructed from satellite imagery, Mon. Wea. Rev., 113, 326-337.

Michaels, P.J., R.A. Pielke, J.T. McQueen, and D.E. Sappington, 1987: Composite climatology of Florida summer thunderstorms, Mon. Wea. Rev., 115, 2781-2791.

McQueen, J.T., and R.A. Pielke, 1985: A numerical climatological investigation of deep convective cloud patterns in south Florida, Atmospheric Science Paper 389, Dept. of Atmospheric Sci., Colorado State University, Ft. Collins, CO 177 pp.

Pielke, R.A., 1974: A three-dimensional numerical model of the sea breezes over south Florida. Mon. Wea. Rev., 102, 115-139.

___, A. Song, P.J. Michaels, W.A. Lyons and R.W. Arritt, 1991: The predictability of sea-breeze generated thunderstorms, Atmosfera, 4, 65-78.

Fig. 1: Cloud frequency composites at 15 (a), 18 (b) and 20 UTC (c) for all days.

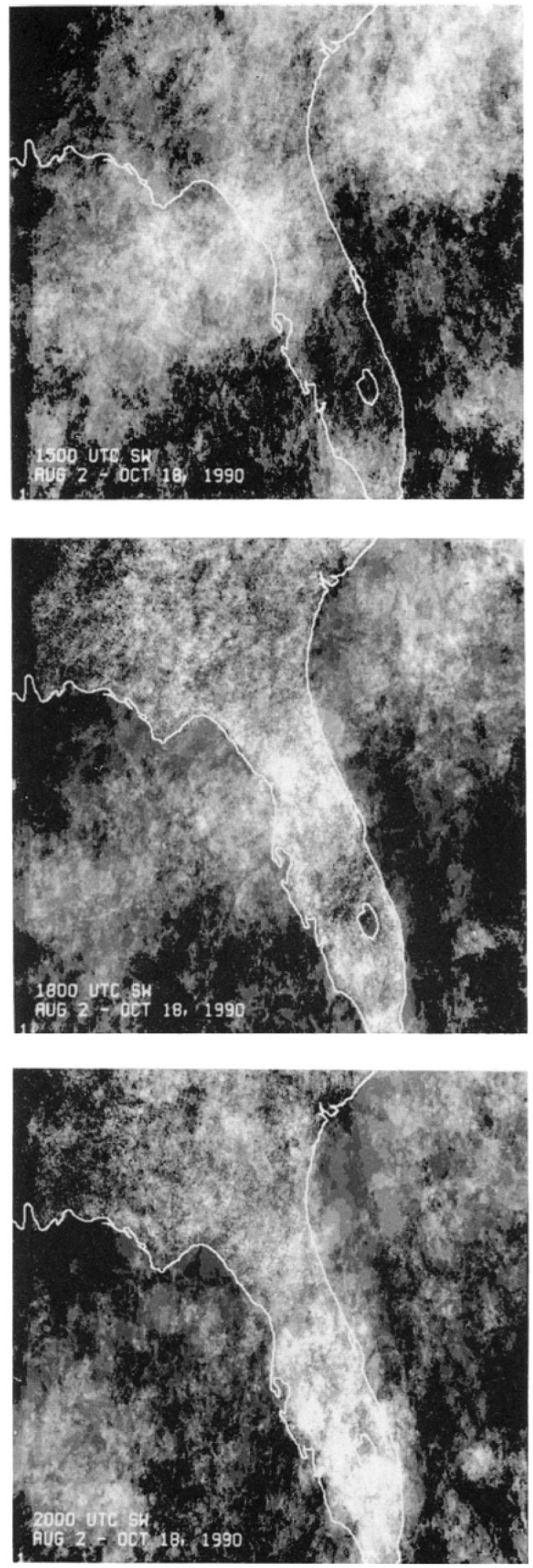

Fig. 2: Cloud frequency composites at 15 (a), 18 (b) and 20 UTC (c) for SW flow days.

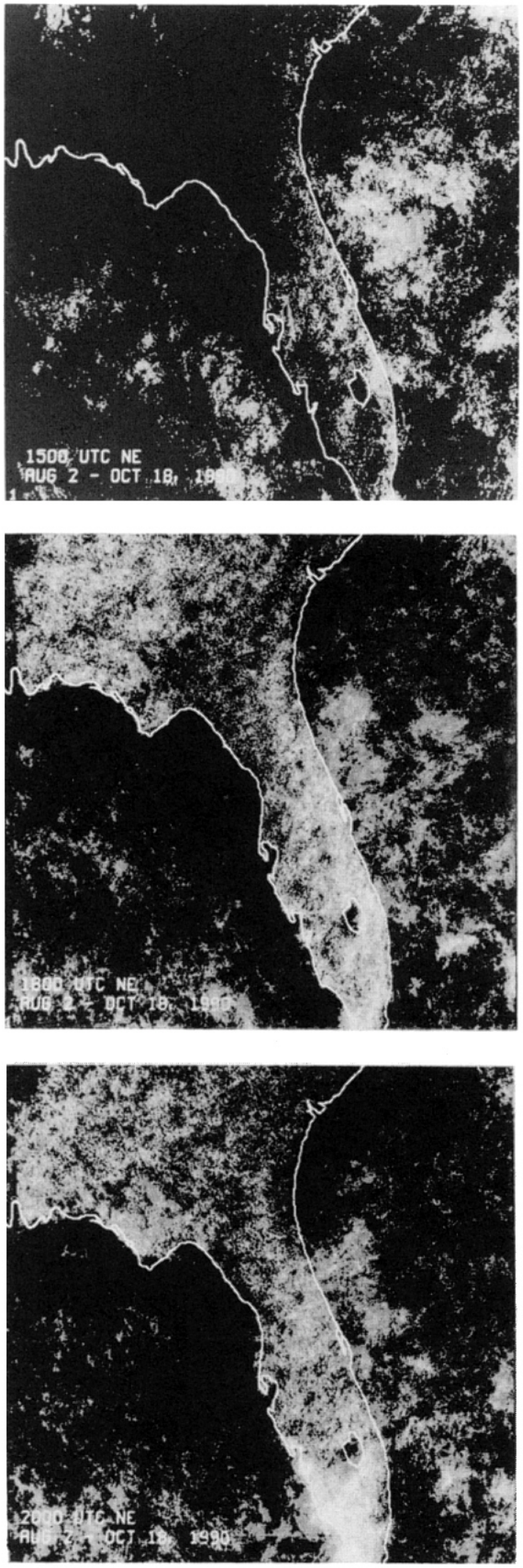

Fig. 3: Cloud frequency composites at 15 (a), 18 (b) and 20 UTC (c) for NE flow days.